Clinical Neurophysiology 130 (2019) 1175–1183

Contents lists available at ScienceDirect

Clinical Neurophysiology

journal homepage: www.elsevier.com/locate/clinph

Simultaneous MEG and EEG to detect ripples in people with focal epilepsy

Nicole van Klink [a,b,*], Anne Mooij [a], Geertjan Huiskamp [a], Cyrille Ferrier [a], Kees Braun [a], Arjan Hillebrand [c], Maeike Zijlmans [a,b]

[a] Brain Center Rudolf Magnus, Department of Neurology and Neurosurgery, UMC Utrecht, the Netherlands
[b] SEIN – Stichting Epilepsie Instellingen Nederland, Heemstede, the Netherlands
[c] Department of Clinical Neurophysiology and Magnetoencephalography Center, VU University Medical Center, Amsterdam, the Netherlands

See Editorial, pages 1172–1174

ARTICLE INFO

Article history:
Accepted 31 January 2019
Available online 23 February 2019

Keywords:
High frequency oscillations
Ripples
Focal epilepsy
Epilepsy surgery
Beamforming
Virtual electrodes

HIGHLIGHTS

- Ripples in MEG and EEG provide complementary information.
- Ripples in MEG are less frequent but more specific for the region of interest than ripples in EEG.
- In sufficient numbers, ripples in EEG and MEG are (partially) concordant with the epileptic region.

ABSTRACT

Objective: We studied ripples (80–250 Hz) simultaneously recorded in electroencephalography (EEG) and magnetoencephalography (MEG) to evaluate the differences.
Methods: Simultaneous EEG and MEG were recorded in 30 patients with drug resistant focal epilepsy. Ripples were automatically detected and visually checked in virtual channels throughout the cortex. The number and location of ripples in EEG and MEG were compared to each other and to a region of interest (ROI) defined by clinically available information.
Results: Eleven patients showed ripples in both MEG and EEG, 11 only in EEG and one only in MEG. Twenty-four percent of the ripples occurred simultaneously in EEG and MEG, 71% only in EEG, and 5% only in MEG. Three patients without spikes in EEG showed EEG ripples. Ripple localization was concordant with the ROI in 80% of patients with MEG ripples, as opposed to 62% full or partial concordance for EEG ripples. With the optimal threshold for localizing the ROI, sensitivity and specificity were more than 80%.
Conclusions: Ripples in MEG are less frequent but more specific and sensitive for the region of interest than ripples in EEG. Ripples in EEG can exist without spikes in the EEG.
Significance: Ripples in MEG and EEG provide complementary information.

1. Introduction

Epilepsy surgery is a treatment option in refractory focal epilepsy. Electroencephalography (EEG) and magnetoencephalography (MEG) are used to non-invasively estimate the location and extent of the so-called epileptogenic zone (i.e., the area that has to be removed during surgery in order to achieve seizure freedom) (Lüders et al., 2006). Routine EEG is performed in most patients, as it is cheap and widely available. The chance of finding epileptiform activity with EEG can be increased by using more electrodes, by recording the EEG after sleep deprivation, or by performing long term (video-)EEG monitoring. MEG is typically used when EEG provides insufficient information. MEG is more expensive and not as widely available as EEG, but it has the advantage that the brain's magnetic fields are not perturbed by the skull, scalp and other

* Corresponding author: University Medical Center Utrecht, Department of Neurology and Neurosurgery, HP C03.131, Heidelberglaan 100, 3584CX Utrecht, the Netherlands.
E-mail address: N.vanklink-2@umcutrecht.nl (N. van Klink).

https://doi.org/10.1016/j.clinph.2019.01.027
1388-2457/

tissues (Cohen and Cuffin, 1983). MEG and EEG can be recorded simultaneously when using MEG-compatible EEG electrodes.

Traditionally, the EEG and MEG recordings are reviewed for the presence of interictal epileptiform discharges such as spikes and sharp waves to provide an estimation of the location of the epileptogenic zone. Studies with simultaneous EEG and MEG recordings have shown that both modalities have their advantages (Baumgartner, 2004; Duez et al., 2016): MEG is more sensitive for superficial sources than EEG, but this reverses at a certain depth. Therefore, MEG shows more spikes in patients with neocortical foci than EEG (Oishi et al., 2002; Ossenblok et al., 2007; Heers et al., 2010), while EEG shows more spikes in (mesial)temporal regions than MEG (Leijten et al., 2003; de Jongh et al., 2005; Iwasaki et al., 2005).

Besides spikes, the analysis of high frequency oscillations (HFOs, 80–500 Hz) has gained interest over the past years, as pathological HFOs in intracranial EEG have shown to be more specific for the epileptogenic zone than spikes (Jacobs et al., 2008; Haegelen et al., 2013). We have recently learned that ripples (80–250 Hz) can be found in non-invasive surface EEG recordings (Andrade-Valenca et al., 2011; Melani et al., 2013; Kobayashi et al., 2015; van Klink et al., 2016b) and MEG (von Ellenrieder et al., 2016; van Klink et al., 2016a; Papadelis et al., 2016; van Klink et al., 2017; Migliorelli et al., 2017; Velmurugan et al., 2018), and that these ripples can be helpful in the identification of the epileptogenic zone, even though the number of ripples in EEG and MEG is lower than in intracranial EEG. One study showed the feasibility of detecting EEG ripples with simultaneously recorded MEG in two cases (Papadelis et al., 2016). We compared the location and number of ripples between both modalities in a larger cohort and compare their value for localizing the epileptogenic focus.

2. Methods

2.1. Patients

We prospectively gathered simultaneous MEG-EEG in 33 patients with pharmacoresistant focal epilepsy, for whom – during the meeting of the UMC Utrecht multidisciplinary epilepsy surgery team – it was decided that MEG could provide additional information for the localization of the epileptogenic focus. Included patients were older than 6 years of age, had no metal implants and were able to lie motionless for at least 15 minutes, which was the minimal duration of one recording epoch. If needed, patients could move between two epochs. Patients were excluded from the analysis if less than 30 minutes of good quality data was available. This study was approved by the medical ethics board of the UMC Utrecht and all patients or their caretakers gave written informed consent.

2.2. Recordings

MEG-EEG data were recorded at the VU Medical Center in Amsterdam, according to the routine clinical protocol. This protocol included approximately 45 minutes of resting state recording, with eyes closed in a supine position. The recording could contain sleep, as patients were sleep deprived and encouraged to sleep during the recording. MEG was recorded with a 306-channel whole-head Elekta system (Elekta Neuromag Oy, Helsinki, Finland) in a magnetically shielded room (VacuumSchmelze GmbH, Hanau, Germany). The MEG system comprised 102 sensor units, each consisting of two orthogonal planar gradiometers and one magnetometer. Five head-localization coils continuously recorded the position of the head relative to the MEG sensors. The data were recorded with a sample frequency of 2500 Hz, and hardware filters at 825 Hz low-pass and 0.1 Hz high-pass. The MEG data were preprocessed by removing the head position coil noise, and temporal extension of signal space separation (tSSS, (Taulu and Hari 2009)) to reduce correlated noise, and cross correlation signal space separation (xSSS, (van Klink et al., 2017)) to reduce uncorrelated noise (Maxfilter, Elekta Neurmag Oy, version 3.0.10). Simultaneous EEG was measured with a 60-channel MEG-compatible EEG cap, (Easycap Gmbh, Herrsching, Germany), with a sample frequency of 2500 Hz, and hardware filters at 600 Hz low-pass and 0.1 Hz high-pass. We selected approximately 30 minutes of resting state signal with few artifacts on visual inspection. The location of the head position coils, the EEG electrodes, and the outline of the head were digitized with a 3D digitizer (Fastrak, Polhemus, Colchester, VT, USA), and co-registered with a previously made T1-weighted structural MRI of each patient. We used surface matching software, developed by one of the authors (AH), to co-register the MRI and MEG-EEG data (Whalen et al., 2008). Patient-specific Boundary Element Model (BEM) volume conductor models were built using OpenMEEG (Gramfort et al., 2010) for MEG and using Dipoli (Oostendorp and van Oostrom 1989) for EEG, using the same scalp, skull and brain meshes, with conductivities for scalp, skull and brain of 0.33, 0.0041, and 0.33 S/m, respectively (Gabriel et al., 1996). We chose two BEM models because we were not able to construct a single BEM model that gave reliable results for both MEG and EEG.

2.3. Data processing

We reconstructed virtual channels for both MEG and EEG to increase the signal to noise ratio. The virtual MEG and EEG signals were calculated with a Synthetic Aperture Magnetometry beamformer (Robinson and Vrba 1999) using the Fieldtrip toolbox (v20170212 (Oostenveld et al., 2011)), with singular value decomposition to determine the optimum current orientation for each location (Sekihara et al., 2004). Virtual channels were positioned in the grey matter of each patient. Grey matter voxels were segmented from the 3D T1 MRI (SPM12), and down sampled to get a minimum inter-channel distance of 5 mm, similar to van Klink et al. (2017). We excluded cerebellar voxels but maintained voxels in deep structures like the hippocampus. This resulted in approximately 2400 voxels per patient, which were used for the reconstruction of virtual channels for both EEG and MEG. The leadfields were normalized per virtual channel to correct for depth dependent amplification of white noise. The data covariance matrix was based on the 80 Hz high-pass filtered MEG and EEG signals. The low pass filter was determined by the anti-aliasing filter. A unity matrix was used as noise covariance. We used a regularization of 5% for both MEG and EEG virtual channels.

2.4. HFO detection

The presence of spikes in the original sensor space data was obtained from the clinical MEG report and determined by consensus of two reviewers (NvK and MZ) for EEG. We analyzed the MEG and EEG source space virtual channels for the presence of ripples by using an adapted version of the HFO detection algorithm of Burnos et al. (2014), with parameters optimized for MEG and EEG separately. This algorithm detects ripples if the amplitude and power in the 80 Hz high pass filtered signal are higher than in the baseline signal, the entropy over the event is stable, and the time-frequency spectrum shows a high frequency component that is spectrally distinct from lower frequency activity. All time instances with at least one virtual channel with a ripple were visually checked, by reviewing maximally three channels with ripples at that time. Only ripple times for which $\geq$2/3 of the reviewed rip-

ples were approved, were used for further analysis, as described in (van Klink et al., 2017). These 'ripple times', time instances for which a ripple was detected in one or more channels, will in the following be referred to as 'ripples'. The identified ripples in MEG and EEG virtual channels (source space) were marked in the original MEG and EEG (sensor space) data and checked one more time for the presence of artifacts. Ripples with an irregular morphology, or co-occurring with an artifact (muscle activity, eye movement) were excluded because they were most likely artifacts. Ripples co-occurring with sleep phenomena were also excluded, as they could be artifacts or physiological ripples. Whilst visually inspecting the original EEG and MEG, we noted for each ripple whether it was also visible in the original sensor space data in the other modality, and whether it co-occurred with a spike in sensor space MEG and/or EEG.

2.5. Spatial distribution analysis

The number of virtual channels that showed ripples was compared between EEG and MEG with a Mann Whitney-U Test. Determining the true spatial extent of ripples in these non-invasive recordings is difficult (Hillebrand and Barnes, 2011); the number of recording electrodes and particularly the spatial dispersion of the beamformer method will highly influence the estimated spatial distribution. To determine the spatial correlation between the EEG and MEG ripples, we determined the number of virtual channels with ripples for both EEG and MEG and subsequently used k-means clustering to identify the different clusters of EEG and MEG ripples in each patient, based on the location of the virtual channel and the number of ripples on that channel. We calculated the distance between the closest MEG and EEG cluster centroids. The optimum number of clusters was determined using the Calinski-Harabasz index (Calinski and Harabasz, 1974). This distance is an indicator of the mismatch between the MEG and EEG ripples.

2.6. Location of ripples

The locations of the virtual EEG and MEG ripples were compared to the region of interest (ROI), as determined by a clinical neurophysiologist, based on the available clinical information, and following the hypothesis of the multi-disciplinary team. This information included (in order of priority): location of successful resective surgery (defined as post-operative seizure freedom at last available follow-up), invasive EEG findings, relevant MRI lesion, non-invasively estimated ROI, based on seizure semiology, non-

Table 1
Patient characteristics.

Pt	Age/ Gender	Interictal EEG	Ictal EEG	MRI	PET	SPECT	Surgery or invasive EEG	ROI (based on)
1	17/F	L CPT	L TPO	No abnormalities	No abnormalities		ECoG L TO, no resection	L CTP (ECoG)
2	16/F	FT L > R	L FT	No abnormalities	L FT & R FP			L FT (EEG)
3	21/F	R T posterior	R TP	No abnormalities	No abnormalities		R T basal, posterior, no seizures	R T (surgery)
4	16/F	F R > L	L FT	No abnormalities	No abnormalities			L FT (ictal EEG)
5	16/M	R TO	R TO	Small white matter abnormality R T basal	R TO		R T, no seizures	R T (surgery)
6	8/M	R TPO	RTPO	White matter loss R TO and L O				R TPO (EEG + MRI)
7	33/F	R T	R CPF	Small white matter lesions			R CP, recurrent seizures of different type	R CP (surgery)
8	26/M	R FT	L and R FT	Mesiotemporal sclerosis R	R T & R F		R T, no seizures	R T (surgery)
9	12/M	R T	R T	Cyste fissura choroidae, developmental venous anomaly L F	Hypometabolism L T		R TO, no seizures	R TO (surgery)
10	17/M	L FT	L F and L T	Prior resection pilocytair astrocytoma, hippocampal sclerosis L		L T	L T, no seizures	L T (surgery)
11	10/M	L C	NA	FCD L F	L F			No ROI (inconsistency)
12	37/F	R FT	R FT	Subtle tissue loss hippocampus R	R T			R T (EEG + MRI + PET)
13	48/F	R TPO	R P	Multiple cavernomas, old resection R TP of AVM				R TPO (EEG + semiology)
14	18/F	L F & L T	L FC	Mesiotemporal sclerosis L	L FT		L T, no seizures	L T (surgery)
15	23/M	P	R P PS	No abnormalities	R F			No ROI (inconsistency)
16	20/F	L FT	L FTC	White matter lesions R FP				No ROI (inconsistency)
17	54/M	R > L F	R F & FT	No abnormalities	No abnormalities			No ROI (inconsistency)
18	21/V	L T	L FT	No abnormalities	No abnormalities			No ROI (inconsistency)
19	14/M	L TP	L FT	No abnormalities	L T		sEEG L insula, no resection	L insula posterior (sEEG)
20	23/M	L TPO	L PO	Extensive tissue damage L PO + L hippocampus and thalamus				L (pre)cuneus (EEG + MRI + semiology)
21	36/F	L > R FC	FC	Polymicrogyria insula L & R + cavernoma pons	R T			L + R insula (MRI + EEG)
22	26/F	L F	L FC	Wallerain degeneration L + hippocampal sclerosis L			L frontal + central disconnection, no seizures	L F (surgery)
23	20/M	L FC	L FC	FCD L F	L F		L F, no seizures	L F (surgery)
24	26/M		L T	No abnormalities	L T			L T (EEG + PET)
25	44/M	R > L T and F	R T & R FC	No abnormalities	R F			R perisylvian (EEG + PET)
26	32/M	R > L FC	R FC	Schizencephaly R P + bilateral FCD			R FC, recurrent seizures	R F inferior (surgery with ECoG)
27	34/M	L CP	L P	Cyste L FP				L CP (EEG + MRI)
28	30/F	L > R FCT	L FCT	No abnormalities	L T	L T	sEEG L TP, no resection	L T (sEEG)
29	19/F	L TPO	PS	Ischemia R and L PO				No ROI (inconsistency)
30	54/M	R & L T	R & L T	Low-grade tumor L F basal	L F basal			L + R T (ictal EEG)

F = female, M = male, L = left, R = right, C = central, P = parietal, T = temporal, F = frontal, O = occipital, PS = parasagittal, FCD = focal cortical dysplasia, AVM = arteriovenous malformation, ECoG = electrocorticography, sEEG = stereo electroencephalography.

invasive video-EEG seizure onset area, abnormalities in positron emission tomography (PET), single-photon emission computed tomography (SPECT), MEG or EEG-fMRI, and interictal video-EEG abnormalities. Patients were excluded from this analysis if no ROI could be defined. When the patient was denied epilepsy surgery or invasive EEG because no hypothesis could be formed, no ROI was defined. We determined concordance by focusing on the core of the ripple cluster: the virtual channels with the highest ripple rates. Ripple locations were considered concordant if the main ripple location was inside the ROI as defined by the clinical neurophysiologist. Ripples were partially concordant if the main focus was partially overlapping the ROI (e.g. temporal ripples with a frontotemporal ROI, or with a temporo-occipital ROI) or if a second (discordant) ripple focus was present. If the focus with the highest ripple rate was outside the ROI, the ripples were considered discordant. We tested the predictive value of ripples to predict good or partial concordance with a receiver operating curve (ROC) with 95% confidence intervals, created with RStudio (version 1.0.143, RStudio Inc, Boston, MA, USA). The cut-off values for EEG and MEG with the highest sensitivity and specificity combination was determined the optimum threshold.

3. Results

3.1. Patients

Thirty-three patients were initially included, of whom three had to be excluded because of poor data quality. The remaining 30 patients were between 8 and 54 years of age (mean 25), and 14 were female. Twelve patients had an epileptogenic MRI abnormality. A summary of clinical findings is presented in Table 1. Twenty-three patients slept during at least 5 minutes of the analyzed recordings. Seventeen patients showed spikes in the sensor space EEG and 20 in the sensor space MEG. Spikes were present in both MEG and EEG in 15 patients, two patients had spikes only in EEG, and five patients had spikes only in MEG. Ten patients had epilepsy surgery, of whom one had recurrent seizures with different semiology, and one had recurrent seizures with the same semiology. The other eight were seizure free (average follow-up 11 months, range 1–32). Two patients underwent invasive EEG recordings, but subsequent resection was not possible. We could not define a ROI in six patients, who were also denied epilepsy surgery for this reason. We reconstructed on average 2367 virtual channels per patient (range: 1825–2899), with an average inter-channel distance of 5.6 mm.

3.2. Ripples

Twenty-three patients showed time instances with ripples ('ripples') in virtual channels. Eleven patients showed ripples in both virtual MEG and EEG channels, eleven patients had ripples in the virtual EEG only, and one patient had ripples only in virtual MEG (Table 2). Some examples of virtual and sensor space ripples are shown in Fig. 1. Most patients showed more EEG than MEG ripples (Fig. 2A). In total, 816 time-instances with virtual ripples were found in the 30 minutes recordings, of which 602 (74%) were only in EEG, 130 (16%) only in MEG, and 84 (11%) occurred simultaneously in EEG and MEG. A median of 11% of the virtual channel EEG ripples were also visible in the sensor space data, compared to 20% of the MEG ripples (Fig. 2C).

Table 2
Results per patient, with the presence of spikes and ripples (R) in EEG and MEG, the location of the core of the ripple cluster, and their concordance to the ROI, the number of ripples simultaneously in MEG and EEG, and the distance between the closest EEG and MEG virtual channel cluster centroids. Ripples were judged to have no focus if virtual channels with ripples were scattered over the brain.

	EEG			MEG			Simultaneous EEG&MEG	
Pt	Spikes in EEG	R in EEG	R in EEG location	Spikes in MEG	R in MEG	R in MEG location	R in MEG and EEG	Cluster distance (mm)
1	Y	57	L PO (+−)	Y	9	L TO (+)	2	41
2	Y	107	L T (+)	Y	133	L T (+)	57	13
3*	Y	0		N	0		0	
4	N	0		N	0		0	
5*	Y	65	R T (+)	Y	11	R T (+)	9	7
6	Y	193	R & L C (−)	Y	1	R TP (+)	0	47
7*	N	0		N	0		0	
8*	N	1	no focus (−)	N	0		0	
9*	Y	34	R TPO (+−)	Y	10	R T (+)	7	14
10*	N	5	L T (+)	Y	2	L P (−)	1	60
11	N	39	F bdz (NA)	N	0		0	
12	Y	2	L T (−)	Y	0		0	
13	N	0		Y	0		0	
14*	N	0		N	0		0	
15	N	18	R & L P (NA)	Y	1	L P (NA)	0	37
16	Y	5	R PO (NA)	Y	0		0	
17	Y	4	no focus (NA)	Y	2	R P (NA)	0	no focus
18	Y	2	L PO (NA)	Y	0		0	
19	Y	36	L TO (+−)	N	0		0	
20	N	2	R & L T (−)	Y	0		0	
21	N	1	R & L T (+−)	N	0		0	
22*	Y	41	L F (+)	Y	29	L F (+)	1	34
23*	Y	5	no focus (−)	Y	0		0	
24	N	0		Y	0		0	
25	Y	0		Y	3	R T (−)	0	
26*	Y	12	R FCP (+−)	Y	4	R C (+)	2	24
27	Y	53	L P (+)	Y	9	L P (+)	5	14
28	Y	0		Y	0		0	
29	N	2	R F (NA)	N	0		0	
30	N	2	no focus (−)	N	0		0	

L = left, R = right, T = temporal, O = occipital, F = frontal, P = parietal, C = central, NA = no region of interest, because of inconsistent clinical information, Y = yes, N = no, +/+−/− = concordance/partial concordance/discordance between ripple and ROI, *Patient was operated.

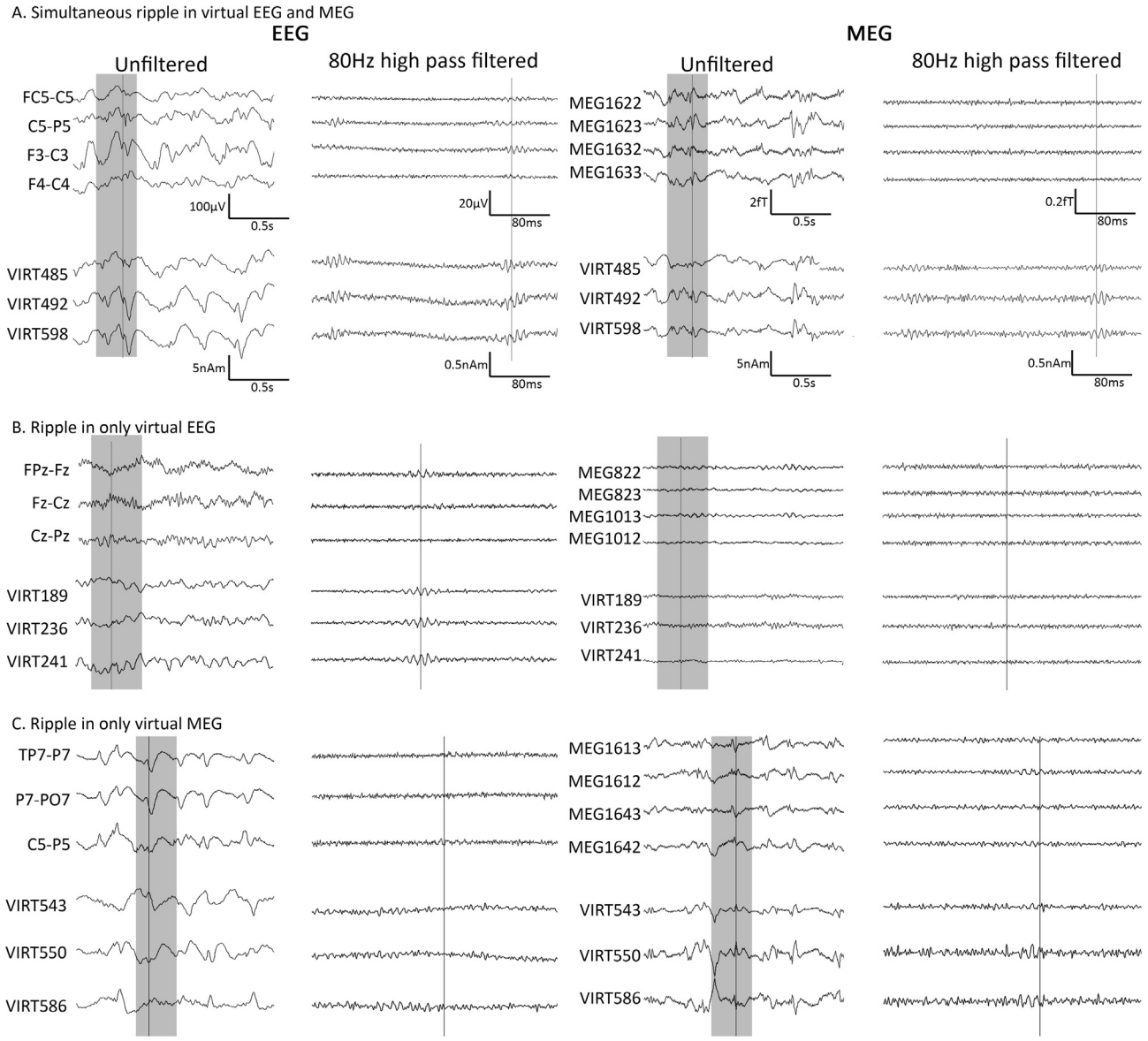

Fig. 1. Examples of EEG and MEG simultaneous sensor data (top) and virtual channels (below). The grey area in the unfiltered signal (left) is shown with 80 Hz high pass filter on the right. The vertical lines represent the same point in time. (A) Example of a ripple, simultaneously occurring in virtual EEG and MEG channels, and also visible in sensor space EEG, but not in sensor space MEG. (B) Example of a ripple without spike in virtual EEG channels and visible in sensor space EEG, but not at MEG sensor space or in virtual MEG channels. (C) Example of a ripple on a spike in virtual MEG channels, maybe visible in sensor space MEG, but not in EEG electrodes or virtual EEG channels. The spike is visible in both sensor space and virtual EEG and MEG.

We sometimes found ripples in EEG sensor data, at the time-point of a virtual MEG ripple, while no virtual EEG ripple was found by the detection algorithm. In such cases we assumed that the virtual EEG ripple was missed by the detector and the ripple occurred simultaneously in MEG and EEG. The other way around – ripples in MEG sensor data at the time-point of a virtual EEG ripple, without virtual MEG ripple – also occurred, and were also marked as 'missed ripples'. Such missed ripples in EEG or MEG were found in 9 patients, and always occurred in patients in whom we had already found ripples in virtual EEG or MEG at other time points. Missed ripples were identified in 9 patients. In six of these patients only one or two ripples were missed. Six ripples were missed in MEG in one patient, 65 were missed in EEG in one patient, and 12 ripples were missed in MEG and 18 in EEG in one patient. If we take these missed ripples into account, 196 of the 816 (24%) ripples occurred simultaneously in MEG and EEG. After correction for 'missed ripples', 71% of the ripples were only visible in EEG, and 5% of the ripples were only visible in MEG (Fig. 2B).

3.3. Ripples and spikes

Eight patients without spikes in EEG showed ripples in EEG and none of the patients without MEG spikes showed MEG ripples. A median of 65% of the EEG ripples co-occurred with EEG spikes and 92% (median) of the MEG ripples co-occurred with MEG spikes (Fig. 2D).

3.4. Spatial distribution

Examples of the spatial distribution of virtual channels with ripples in EEG and MEG are shown in Fig. 3. Ripples in EEG covered more virtual channels than ripples in MEG (Fig. 2E, median 23% vs. 2% of the virtual channels contained ripples, $U = 70.5$, $p = 0.025$). In patients with both MEG and EEG ripples, on average 75% of the virtual channels with MEG ripples also showed EEG ripples, whereas on average 9% of the virtual channels with EEG ripples also showed MEG ripples. The median distance between the

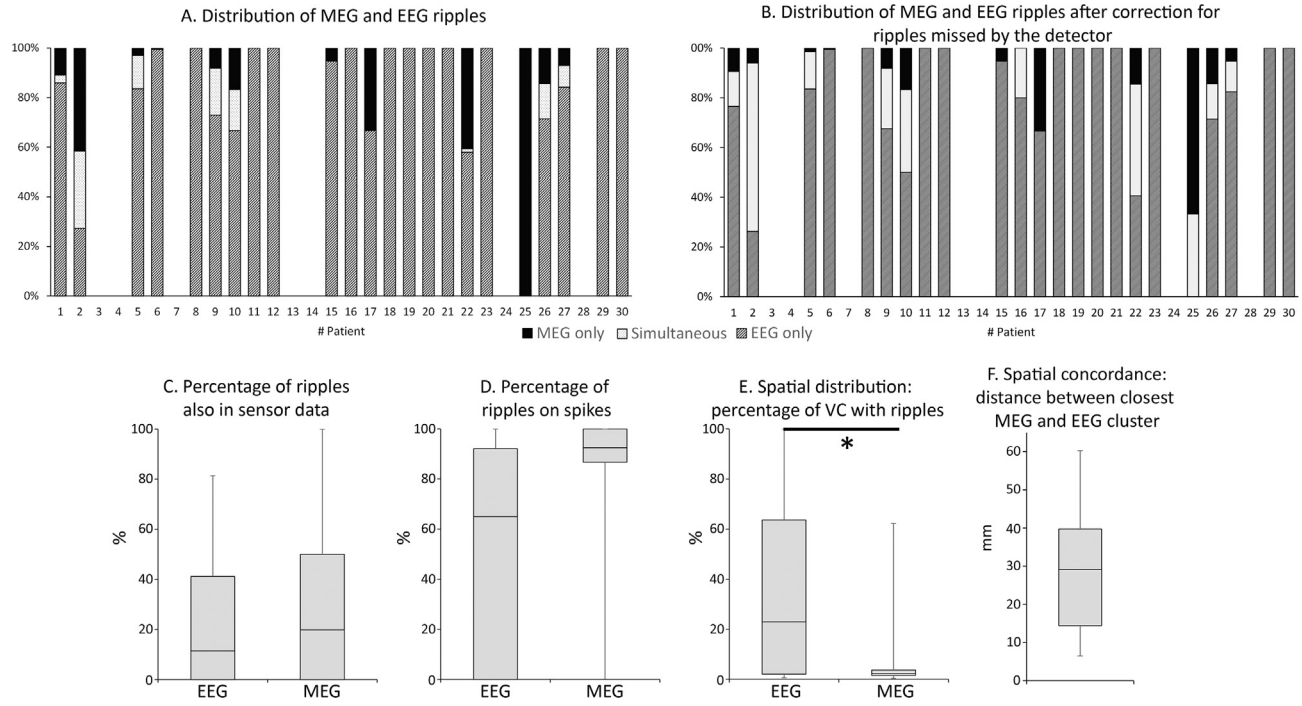

Fig. 2. (A) Distribution of number of MEG, EEG and simultaneous ripples in each patient. Most patients (21/22, 95%) showed more EEG than MEG ripples. Only 10% of the ripples were simultaneously detected in MEG and EEG, before correction for ripples missed by the detection algorithm. (B) After correction of ripples that were missed by the detector, 24% of the ripples were simultaneously visible in MEG and EEG. (C) Boxplot of the percentage of virtual EEG and MEG ripples that were also visible in the sensor space EEG and MEG data, respectively. (D) Boxplot of the percentage of EEG and MEG ripples that co-occurred with a spike in the EEG and MEG sensor space data, respectively. (E) Boxplot showing the spatial distribution by means of the percentage of virtual channels (VC) that showed EEG and MEG ripples. EEG ripples were found in more virtual channels than MEG ripples ($^{*}p = 0.025$). (F) Boxplot showing the spatial concordance between MEG and EEG ripples by means of the distance between closest MEG and EEG virtual channel clusters.

closest EEG and MEG clusters was 29 mm (Fig. 2F), indicating that they often pointed to the same lobe.

3.5. Location of ripples

In 6 patients we could not estimate the ROI. The location of EEG ripples was concordant with the ROI in 5 of the remaining 16 patients (31%) with EEG ripples, partially concordant in 5 patients (31%), and not concordant in 7 patients (43%). The location of MEG ripples was concordant with the ROI in 8 of the 10 patients with MEG ripples (80%), and not concordant in 2 patients (20%). The ROC curve with the predictive value of EEG and MEG ripples is shown in Fig. 4. The optimum threshold for EEG ripples was >8, so if more than 8 ripples were detected, the ROI was at least partially concordant with a sensitivity of 80% and specificity of 83%. The optimum threshold for MEG ripples was >3, with a sensitivity of 88% and a specificity of 100%.

When only considering the 12 patients with >8 EEG ripples, the location of the ripples was concordant in 5 and partially concordant in 4 patients, 2 patients had no ROI. For the one patient with more than 8 ripples (patient 6) that were not concordant with the ROI, the MEG and EEG ripples were concordant and mostly co-occurring with the MEG and EEG spikes in this recording, but not with other investigations. Seven patients showed or >3 MEG ripples, and their location was always concordant with the ROI.

Of the ten patients who underwent surgery (patients 3, 5, 7, 8, 9, 10, 14, 22, 23 and 26), three did not show ripples in EEG or MEG. Three patients showed few EEG ripples, subthreshold, and one of them also showed 2 MEG ripples. Patients 5, 9, 22 and 26 showed above-threshold ripples in EEG and MEG which were concordant with the resection. In patient 9 the main EEG ripple focus was in the ROI, but extended outside of it, so it was scored as partial concordance.

Interestingly, three patients without spikes in the EEG (patients 10, 11 and 15) showed ripples in EEG that were concordant with other clinical findings. Patient 10 showed most EEG ripples in the left temporal lobe, concordant with the MEG spikes, and with the resection after successful surgery. Patient 11 showed bilateral frontal ripples in the EEG, concordant with abnormal beta activity found in this region in EEG and MEG, and the FCD found on MRI. Patient 15 showed bilateral parasagittal parietal EEG ripples that were partially concordant with the left parietal MEG spikes and part of the large epileptogenic region that was found with ictal EEG. The five other patients without spikes in the EEG showed few (a maximum of 2) ripples in the EEG, which were not concordant with the ROI.

4. Discussion

We showed that ripples can be identified in simultaneously recorded EEG and MEG, and only 24% of these ripples were simultaneously visible in both modalities. The yield of ripples was substantially increased using beamformer virtual channels. EEG revealed more ripples than MEG and showed ripples that could localize the region of interest even in patients without spikes. Ripples found in MEG seemed more specific. EEG and MEG ripples were predictive for the region of interest when present in sufficient numbers: the presence of more than 8 EEG ripples indicated the ROI with sensitivity of 80% and specificity of 83%, and presence of more than 3 MEG ripples indicated the ROI with sensitivity of 88% and specificity of 100%.

One study in two patients has previously shown the feasibility of detecting ripples in simultaneously recorded MEG-EEG, where the analysis was restricted to ripples co-occurring with spikes (Papadelis et al., 2016). We have shown here that the minority of

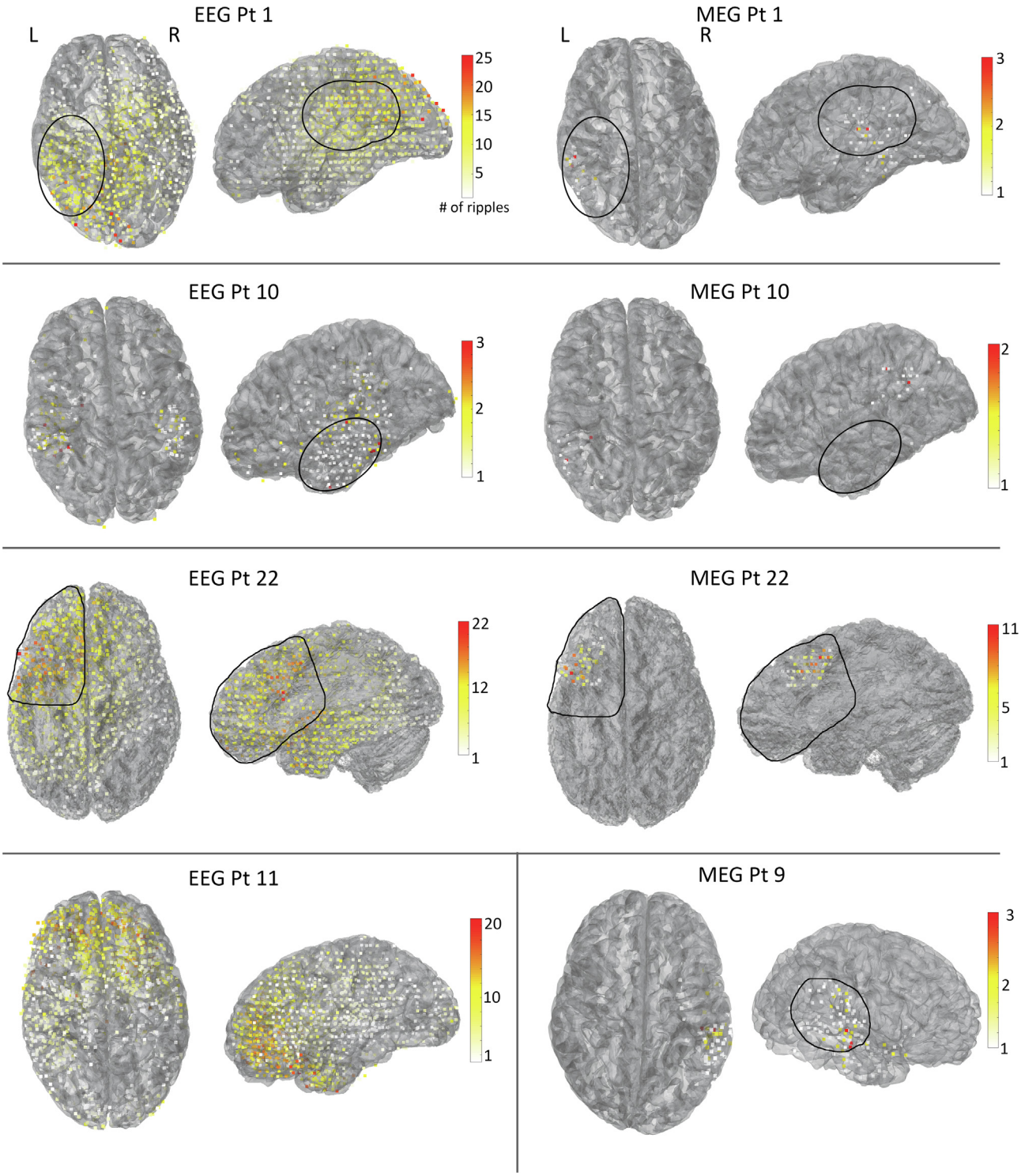

Fig. 3. Examples of EEG and MEG ripples in 3 patients, and EEG ripples in 2 patients. Each colored dot is a virtual channel, with the number of ripples on that channel in a color scale from white (1) via yellow (half maximum) to red (maximum in that modality in that patient). The region of interest as defined by the clinical neurophysiologist is delineated in black. Patient 1 shows a large EEG ripple focus left parieto-occipital (partially concordant with ROI), and MEG ripples left temporo-occipital (concordant). Patient 10 the most prominent EEG ripple focus left temporal (concordant). MEG ripples were found in the left parietal area (not concordant). Patient 22 shows a large area with EEG ripples most prominent left frontal, which is also the location of the MEG ripples, which were more focal (both concordant). Patient 11 shows bilateral frontal EEG ripples (no ROI could be defined, concordant with MEG spikes). This patient did not show EEG spikes, nor MEG ripples. Patient 9 shows MEG ripples right temporo-parietal (concordant).

the ripples in EEG and MEG occur simultaneously. Assessing ripples in both MEG and EEG therefore increases the amount of information about the epileptogenic zone. Another study compared rates of ripples in MEG and EEG, although not measured simultaneously (von Ellenrieder et al., 2016). Like our results, they found higher rates of ripples in EEG than in MEG, and MEG ripples were detected in a subset of patients with EEG ripples. We hypothesize that the lower number of MEG ripples is mainly related to the differences in noise characteristics in MEG and EEG. For example MEG is more sensitive to environmental background noise, while EEG is

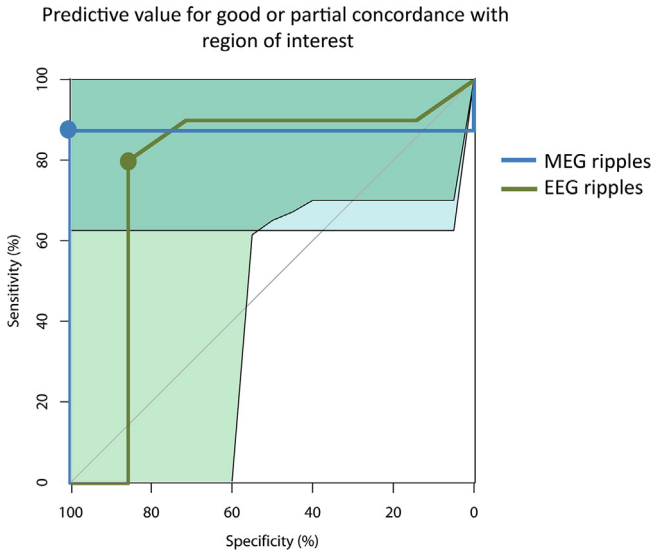

Fig. 4. Predictive value of EEG (blue) and MEG (green) ripples for good or partial concordance with the ROI. The 95% confidence intervals are indicated in light green for EEG ripples, light blue for MEG ripples, and darker green-blue when overlapping. The highest sensitivity and specificity combinations were considered the optimum threshold. This threshold was more than 8 for EEG ripples, with a sensitivity of 80% and a specificity of 83% (green dot). For MEG the threshold was more than 3 ripples, with a sensitivity of 88% and a sensitivity of 100% (blue dot).

more sensitive to EMG artifacts. The amount of sleep, and therefore decrease of noise, could have influenced the number of ripples found in the selected epochs. We did not differentiate between ripples in sleep or in wake in this study. Previous studies have shown that ripples in surface EEG and MEG co-occur with spikes for 80–94% of the ripples (Andrade-Valenca et al., 2011; von Ellenrieder et al., 2016). These numbers are in line with our findings for MEG, with 92% of ripples co-occurring with a spike. Only 65% of our ripples in EEG co-occurred with a spike, which is mainly explained by the observation that some patients had ripples but no spikes. When the three patients with most ripples but without spikes (those discussed in the last paragraph of the Results section) were left out, 85% of the ripples in EEG co-occurred with a spike. The fact that spikes can be invisible in MEG or EEG, based on spatial extent and synchronicity over gyri and sulci, could also play a role. If a similar dipole generator is assumed for ripples, this could result in a difference in spatial extent and therefore synchronicity between spikes and ripples. We included patients with and without spikes in EEG or MEG, while studies so far have only focused on patients with spikes. Interestingly, our series show three patients without spikes but with ripples in the EEG, concordant with the other clinical information. These are the patients in whom ripple analysis can offer important added value. MEG did not show ripples in patients without MEG spikes.

Ripples that do not co-occur with spikes could be physiological, or artifacts. Physiological ripples in surface EEG have been described during sleep, particularly related to sleep phenomena (Mooij et al., 2017). Artifactual ripples exist most often in the frontal channels, associated with eye movements, or in temporal channels, caused by muscle activity. Although we cannot guarantee that our ripples without spikes were truly epileptogenic, we checked the raw unfiltered EEG and MEG channels carefully and excluded ripples co-occurring with sleep phenomena, and ripples suspect for artifacts because of muscle activity or eye movement. The concordance or partial concordance with the ROI suggests that the ripples in this study are at least in majority pathological.

Both EEG and MEG ripples that were present in small numbers did not show concordance with the region of interest. These ripples are most likely not epileptogenic, and probably artifacts. This warrants us to be careful when drawing clinical conclusions on non-invasive ripple analysis. This is comparable to interictal spikes which can be non-specific, if not present at considerable rates.

We used beamformer virtual channels in EEG and MEG to increase the signal-to-noise ratio (SNR), specifically in the high frequency band (van Klink et al., 2016a). Only 11% and 20% of the virtual EEG and MEG ripples, respectively, were also visible in the original sensor data, indicating that the virtual channels increase the yield substantially by attenuating the noise. Calculating the beamformer virtual channels and subsequent automatic ripple detection in the 2367 channels is a time-consuming procedure, but this is mainly computational time which can be reduced by optimal parallel computing. This step of reconstructing beamformer virtual channels is only used to identify the time-points with ripples. One way to reduce the number of virtual channels is to place them iteratively (Migliorelli et al., 2017). If we can further improve the SNR of the MEG and EEG signals by other means, e.g. better recording systems, more low-noise circumstances, or better post-processing, the yield of ripples in sensor space data can increase and calculation beamformer virtual channels might not be necessary.

A limitation of this study is that the true epileptogenic zone might differ from the region of interest as estimated here. In our center, MEG is only used for the presurgical evaluation of complex cases in whom there is uncertainty about the epileptogenic zone based on video-EEG, semiology and neuroimaging, because these investigations were non-informative or yielded discordant results. This is reflected in the presence of an epileptogenic lesion in only 12 of 30 patients. The epileptogenic zone was confirmed in eight patients who had successful surgery (i.e. patients were seizure free postoperatively), but in most patients the work-up for surgery was still ongoing or surgery was considered not feasible. Ripple analysis needs to be performed in a larger group of patients with known postoperative seizure outcome to determine the sensitivity and specificity of ripples accurately. Comparing non-invasive ripples with invasive HFOs would be an alternative approach to determine the value of non-invasive ripples.

To be able to analyze ripples in such a large number of virtual channels, we relied on an automatic detection algorithm that was optimized before separately on MEG virtual channel data (van Klink et al., 2017) and EEG virtual channel data (unpublished). Optimization was performed with a preference towards high sensitivity, while restricting the number of false positives. A visual check was used to further minimize the false positives, but false negatives were not systematically assessed. During visual check of the raw MEG and EEG signal, we found missed ripples in nine patients, of whom in 3 patients the detector missed more than 2 ripples. These findings changed the number of co-occurring ripples in MEG and EEG (24% with missed ripples vs. 11% without), and were therefore reported. This unique way of checking detector accuracy in such a large dataset showed that the algorithm did not perform optimally in three patients, which is a drawback of any automatic detection algorithm. The missed ripples were only taken into account in determining the co-occurrence of MEG and EEG ripples, and not in the spatial distribution analysis and comparison with the ROI, because their location with respect to the virtual channels was unknown. The numbers of missed ripples was small compared to the total number in each patient, and most likely does not affect the other analyses.

A second limitation is that the comparison of the localization of ripples in EEG and MEG was hindered by the difference in spatial resolution between the techniques. With 306 MEG sensors the MEG coverage was much more comprehensive than that offered by 60 EEG electrodes. This might explain the broad coverage of virtual electrodes with EEG ripples and therefore the decreased sensitivity compared to MEG ripples. The poorer resolution could also be

attributed to the volume conduction of the skull and scalp that affect EEG much more than MEG. Despite the lower spatial resolution of EEG, we found more EEG than MEG ripples. We assume that the higher signal-to-noise ratio of the 80 Hz high pass filtered EEG compared to the 80 Hz high pass filtered MEG is the main cause of this. With ripples spread out over more virtual channels in EEG than MEG, the chance of missing a ripple was lower in EEG. We tried to minimize this by oversampling the brain with virtual channels every 5 mm, which should be in the order of the spatial resolution of the MEG virtual channels (van Klink et al., 2016a). Fusion of MEG and EEG data, as has also been proposed for spike analysis (Baumgartner 2004; Ossenblok et al., 2007; Aydin et al., 2014), by calculating one set of virtual channels based on the combined MEG and EEG data, might result in an improved SNR and spatial resolution of the virtual channels, and therefore might reveal more, and more accurate, ripples than for the separate techniques. Some studies have shown that MEG might be better to identify spikes in neocortical foci than EEG (Oishi et al., 2002; Ossenblok et al., 2007; Heers et al., 2010). To investigate if this is similar for ripples, we need a more homogenous study population with known pathology.

5. Conclusion

This study shows the potential of ripple analysis in non-invasive EEG and MEG. When ripples in MEG were found, their sensitivity and specificity for the region of interest was high. Ripples in EEG were found in more patients and higher numbers and can be found in patients without interictal spikes. The value of ripple analysis over spike analysis must be confirmed in studies investigating their localization sensitivity and specificity compared to the epileptogenic zone in patients after successful surgery.

Conflict of interest statement

None of the authors have potential conflicts of interest to be disclosed.

Acknowledgements

This manuscript was supported by the Dutch Brain Foundation (number 2013-139) and the Dutch Epilepsy Foundation 15-09. M. Zijlmans is supported by ZonMW veni 91615149. The authors would like to thank Nico Akemann, Ndedi Sijsma, Karin Plugge, Marieke Alting Siberg and Peterjan Ris for the technical assistance and the clinical MEG analyses.

References

Andrade-Valenca LP, Dubeau F, Mari F, Zelmann R, Gotman J. Interictal scalp fast oscillations as a marker of the seizure onset zone. Neurology 2011;77:524–31.
Aydin U, Vorwerk J, Kupper P, Heers M, Kugel H, Galka A, et al. Combining EEG and MEG for the reconstruction of epileptic activity using a calibrated realistic volume conductor model. PLoS One 2014;9:e93154.
Baumgartner C. Controversies in clinical neurophysiology. MEG is superior to EEG in the localization of interictal epileptiform activity. Con. Clin Neurophysiol. 2004;115:1010–20.
Burnos S, Hilfiker P, Sürücü O, Scholkmann F, Krayenbühl N, Grunwald T, et al. Human intracranial high frequency oscillations (HFOs) detected by automatic time-frequency analysis. PLoS One. 2014;9:e94381.
Calinski R, Harabasz J. A dendrite method for cluster analysis. Commun. Stat. 1974;3:1–27.
Cohen D, Cuffin BN. Demonstration of useful differences between magnetoencephalogram and electroencephalogram. Electroencephalogr. Clin. Neurophysiol. 1983;56:38–51.
de Jongh A, de Munck JC, Gonçalves SI, Ossenblok P. Differences in MEG/EEG epileptic spike yields explained by regional differences in signal-to-noise ratios. J. Clin. Neurophysiol. 2005;22:153–8.
Duez L, Beniczky S, Tankisi H, Hansen PO, Sidenius P, Sabers A, et al. Added diagnostic value of magnetoencephalography (MEG) in patients suspected for epilepsy, where previous, extensive EEG workup was unrevealing. Clin. Neurophysiol. 2016;127:3301–5.
Gabriel S, Lau RW, Gabriel C. The dielectric properties of biological tissues: II. Measurements in the frequency range 10 Hz to 20 GHz. Phys. Med. Biol. 1996;41(11):2251–69. https://doi.org/10.1088/0031-9155/41/11/002.
Gramfort A, Papadopoulo T, Olivi E, Clerc M. OpenMEEG: opensource software for quasistatic bioelectromagnetics. Biomed. Eng. Online 2010;9:45.
Haegelen C, Perucca P, Châtillon C-E, Andrade-Valença L, Zelmann R, Jacobs J, et al. High-frequency oscillations, extent of surgical resection, and surgical outcome in drug-resistant focal epilepsy. Epilepsia 2013;54:848–57.
Heers M, Rampp S, Kaltenhäuser M, Pauli E, Rauch C, Dölken MT, et al. Detection of epileptic spikes by magnetoencephalography and electroencephalography after sleep deprivation. Seizure 2010;19:397–403.
Hillebrand A, Barnes GR. Practical constraints on estimation of source extent with MEG beamformers. Neuroimage 2011;54:2732–40.
Iwasaki M, Pestana E, Burgess RC, Lüders HO, Shamoto H, Nakasato N. Detection of epileptiform activity by human interpreters: blinded comparison between electroencephalography and magnetoencephalography. Epilepsia 2005;46:59–68.
Jacobs J, LeVan P, Chander R, Hall J, Dubeau F, Gotman J. Interictal high-frequency oscillations (80–500 Hz) are an indicator of seizure onset areas independent of spikes in the human epileptic brain. Epilepsia 2008;49:1893–907.
Kobayashi K, Akiyama T, Oka M, Endoh F, Yoshinaga H. A storm of fast (40–150 Hz) oscillations during hypsarrhythmia in West syndrome. Ann. Neurol. 2015;77:58–67.
Leijten FSS, Huiskamp G-JM, Van Hilgersom I, Huffelen AC. High-resolution source imaging in mesiotemporal lobe epilepsy: a comparison between MEG and simultaneous EEG. J. Clin. Neurophysiol. 2003;20:227–38.
Lüders HO, Najm I, Nair D, Widdess-Walsh P, Bingman W. The epileptogenic zone: general principles. Epileptic Disord. 2006;8:S1–9.
Melani F, Zelmann R, Dubeau F, Gotman J. Occurrence of scalp-fast oscillations among patients with different spiking rate and their role as epileptogenicity marker. Epilepsy Res. 2013;106:345–56.
Migliorelli C, Alonso J, Romero S, Nowak R, Russi A, Mananas M. Automated detection of epileptic ripples in MEG using beamformer-based virtual sensors. J. Neural Eng. 2017;14:046013.
Mooij AH, Raijmann RCMA, Jansen FE, Braun KPJ, Zijlmans M. Physiological ripples (±100 Hz) in spike-free scalp EEGs of children with and without epilepsy. Brain Topogr. 2017;30:739–46.
Oishi M, Otsubo H, Kameyama S, Morota N, Masuda H, Kitayama M, et al. Epileptic spikes: magnetoencephalography versus simultaneous electrocorticography. Epilepsia 2002;43:1390–5.
Oostendorp TF, van Oostrom A. Source parameter estimation in inhomogeneous volume conductors of arbitrary shape. IEEE Trans. Biomed. Eng. 1989;36:382–91.
Oostenveld R, Fries P, Maris E, Schoffelen J-M. FieldTrip: open source software for advanced analysis of MEG, EEG, and invasive electrophysiological data. Comput. Intell. Neurosci. 2011;2011:1–9.
Ossenblok P, De Munck JC, Colon A, Drolsbach W, Boon P. Magnetoencephalography is more successful for screening and localizing frontal lobe epilepsy than electroencephalography. Epilepsia 2007;48:2139–49.
Papadelis C, Tamilia E, Stufflebeam S, Grant PE, Madsen JR, Pearl PL, et al. Interictal high frequency oscillations detected with simultaneous magnetoencephalography and electroencephalography as biomarker of pediatric epilepsy. J. Vis. Exp. 2016;e54883:1–13.
Robinson S, Vrba J. Functional neuroimaging by synthetic aperture magnetometry (SAM). In: Yoshimoto T, Kotani M, Kuriki S, Karibe H, Nakasato N, editors. Recent Advances in Biomagnetism. Sendai: Tohoku University Press; 1999. p. 302–5.
Sekihara K, Nagarajan SS, Poeppel D, Marantz A. Asymptotic SNR of scalar and vector minimum-variance beamformers for neuromagnetic source reconstruction. IEEE Trans. Biomed. Eng. 2004;51:1726–34.
Taulu S, Hari R. Removal of magnetoencephalographic artifacts with temporal signal-space separation: demonstration with single-trial auditory-evoked responses. Hum Brain Mapp. 2009;30:1524–34.
van Klink NE, Hillebrand A, Zijlmans M. Identification of epileptic high frequency oscillations in the time domain by using MEG beamformer-based virtual sensors. Clin. Neurophysiol. 2016a;127:197–208.
van Klink NEC, van 't Klooster MA, Leijten FSS, Jacobs J, Braun KPJ, Zijlmans M. Ripples on rolandic spikes: a marker of epilepsy severity. Epilepsia 2016b;57:1179–89.
van Klink N, van Rosmalen F, Nenonen J, Burnos S, Helle L, Taulu S, et al. Automatic detection and visualisation of MEG ripple oscillations in epilepsy. NeuroImage Clin. 2017;15:689–701.
Velmurugan J, Nagarajan SS, Mariyappa N, Ravi SG, Thennarasu K, Mundlamuri RC, et al. Magnetoencephalographic imaging of ictal high-frequency oscillations (80–200 Hz) in pharmacologically resistant focal epilepsy. Epilepsia 2018;1:190–202.
von Ellenrieder N, Pellegrino G, Hedrich T, Gotman J, Lina JM, Grova C, et al. Detection and magnetic source imaging of fast oscillations (40–160 Hz) recorded with magnetoencephalography in focal epilepsy patients. Brain Topogr. 2016;29:218–31.
Whalen C, Maclin EL, Fabiani M, Gratton G. Validation of a method for coregistering scalp recording locations with 3D structural MR images. Hum. Brain Mapp. 2008;29:1288–301.